Joint Spectral and Spatial Preprocessing Prior to Endmember Extraction from Hyperspectral Images

Gabriel Martín[a] and Antonio Plaza[a]

[a]Hyperspectral Computing Laboratory
Department of Technology of Computers and Communications
University of Extremadura, Avda. de la Universidad s/n
10071 Cáceres, Spain

ABSTRACT

Hyperspectral unmixing is a very important task for remotely sensed hyperspectral data exploitation. It amounts at estimating the abundance of pure spectral signatures (called endmembers) in each mixed pixel of the original hyperspectral image, where mixed pixels arise due to insufficient spatial resolution and other phenomena. A challenging problem in spectral unmixing is how to automatically derive endmembers from hyperspectral images, particularly due to the presence of mixed pixels which generally prevents the localization of pure spectral signatures in transition areas between different land-cover classes. A possible strategy to address this problem is to guide the endmember extraction process to spatially homogeneous areas. For this purpose, several preprocessing methods (intended to be applied prior to the endmember extraction stage) have been developed in the literature. However, most of these methods only include spatial information during the preprocessing and disregard spectral information until the subsequent endmember extraction stage. In this paper, we develop a new joint spatial and spectral preprocessing method which can be combined with any endmember extraction algorithm from hyperspectral images. The proposed method is intended to retain spectrally pure pixels which belong to spatially homogeneous areas. Our assumption is that spectrally pure signatures are more likely to be found in spatially homogeneous areas rather than in transition areas between different land-cover classes, which are expected to be dominated by mixed pixels. Our experimental results, conducted with a variety of hyperspectral images, reveal the robustness of the proposed method when compared to other similar preprocessing strategies.

Keywords: Hyperspectral image analysis, endmember extraction, spectral unmixing, spatial preprocessing, spatial-spectral preprocessing.

1. INTRODUCTION

Spectral mixture analysis (also called *spectral unmixing*) has been an alluring exploitation goal from the earliest days of hyperspectral imaging[1] to our days.[2,3] No matter the spatial resolution, the spectral signatures collected in natural environments are invariably a mixture of the signatures of the various materials found within the spatial extent of the ground instantaneous field view of the imaging instrument.[4] The availability of hyperspectral imagers with a number of spectral bands that exceeds the number of spectral mixture components[5] has allowed to cast the unmixing problem in terms of an over-determined system of equations in which, given a set of pure spectral signatures (called *endmembers*) the actual unmixing to determine apparent pixel *abundance fractions* can be defined in terms of a numerical inversion process.[6]

A standard technique for spectral mixture analysis is *linear* spectral unmixing,[7] which assumes that the collected spectra at the spectrometer can be expressed in the form of a linear combination of endmembers weighted by their corresponding abundances. Over the few years, many techniques have been developed for spectral-based endmember extraction[8,9] but only a few methods have been designed under the assumption that spatial information can help in the process of extracting spectral endmembers. Techniques include automatic morphological endmember extraction (AMEE),[10] spatial-spectral endmember extraction (SSEE),[11] spatial preprocessing (SPP)

Send correspondence to Antonio J. Plaza:
E-mail: aplaza@unex.es; Telephone: +34 927 257000 (Ext. 51662); URL: http://www.umbc.edu/rssipl/people/aplaza

using a sliding-window approach,[12] and a region-based spatial preprocessing (RBSPP) approach.[13] The first two approaches are endmember extraction algorithms themselves, while the latter two approaches are preprocessing modules that can be combined with any other spectral-based endmember extraction algorithm. Although these approaches have been shown in previous work to be effective in spatial-spectral characterization prior to spectral unmixing, their performance is generally sensitive to noise. Further, these approaches treat the spatial and the spectral information separately, but in some cases fusing both sources of information when performing the preprocessing can be beneficial in order to avoid discarding important information.

In this work, we discuss a noise-robust spatial preprocessing (NRSPP) module which can be used in combination with available endmember extraction algorithms and which fuses both spatial and spectral information at the preprocessing level. The method first derives a spatial homogeneity index which is relatively insensitive to the noise present in the original hyperspectral data. Then, it fuses this index with a spectral-based unsupervised clustering technique, obtaining a set of pure regions which are used to guide the subsequent endmember searching process, which can be conducted using any traditional algorithm for endmember extraction. The remainder of the abstract is organized as follows. Section 2 describes related work, including spectral and spatial-spectral based techniques for endmember extraction. In section 3, we describe the proposed method in step-by-step fashion using a synthetic hyperspectral image to illustrate the outcome of each step. In section 4, we provide an experimental comparison of the proposed method with other spatial-spectral approaches such as AMEE, SSEE, SPP and RBSPP using both synthetic and real hyperspectral data collected by the Airborne Visible Infra-Red Imaging Spectrometer (AVIRIS).[5] This section also discusses future research avenues.

2. RELATED WORK

In this section, we describe in more detail a selected spectral-based endmember extraction algorithm called orthogonal subspace projection (OSP),[14] two spatial-spectral endmember extraction algorithms (AMEE, SSEE) and two spatial preprocessing techniques (SPP and RBSPP) that will be used in our comparison in this paper. The reasons for our selection are: 1) the OSP algorithm represents a class of convex geometry-based and techniques which have been successful in endmember extraction; 2) the AMEE and SSEE are two of few algorithms designed to consider simultaneously the spectral and spatial information in the search for endmembers; and 3) the SPP and RBSPP are the only two spatial preprocessing algorithms prior to endmember extraction available in the literature. These techniques will be compared with our newly developed NRSPP method in this work.

2.1 Orthogonal subspace projection (OSP)

This algorithm starts by selecting the pixel vector with maximum length in the scene as the first endmember. Then, it looks for the pixel vector with the maximum absolute projection in the space orthogonal to the space linearly spanned by the initial pixel, and labels that pixel as the second endmember. A third endmember is found by applying an orthogonal subspace projector to the original image,[14] where the signature that has the maximum orthogonal projection in the space orthogonal to the space linearly spanned by the first two endmembers. This procedure is repeated until a desired number of endmembers are found.[15]

2.2 Automatic Morphological Endmember Extraction (AMEE)

The automatic morphological endmember extraction (AMEE)[10] algorithm runs on the full data cube with no dimensional reduction, and begins by searching spatial neighborhoods around each pixel vector in the image for the most spectrally pure and mostly highly mixed pixel. This task is performed by using extended mathematical morphology operators[16] of dilation and erosion, where dilation selects the most spectrally pure pixel in a local neighborhood around each pixel vector and erosion selects the most highly mixed pixel in the same neighborhood. Each spectrally pure pixel is then assigned an *eccentricity* value, which is calculated as the spectral angle distance (SAD)[6,17] between the most spectrally pure and mostly highly mixed pixel for each given spatial neighborhood. This process is repeated iteratively for larger spatial neighborhoods up to a maximum size that is pre-determined. At each iteration the eccentricity values of the selected pixels are updated. The final endmember set is obtained by applying a threshold to the resulting greyscale eccentricity image, which results in a large set of endmember candidates. The final endmembers are extracted after applying the OSP method to the set of candidates in order to derive a final set of spectrally distinct endmembers, where the number of endmembers to be found is an input parameter to the OSP algorithm.

2.3 Spatial Spectral Endmember Extraction (SSEE)

The spatial-spectral endmember extraction tool (SSEE) uses spatial constraints to improve the relative spectral contrast of endmember spectra that have minimal unique spectral information, thus improving the potential for these subtle, yet potentially important endmembers, to be selected. With SSEE, the spatial characteristics of image pixels are used to increase the relative spectral contrast between spectrally similar, but spatially independent endmembers. The SSEE algorithm searches an image with a local search window centered around each pixel vector and comprises four steps.[11] First, the singular value decomposition (SVD) transform is applied to determine a set of eigenvectors that describe most of the spectral variance in the window or partition. Second, the entire image data are projected onto the previously extracted eigenvectors to determine a set of candidate endmember pixels. Then, spatial constraints are used to combine and average spectrally similar candidate endmember pixels by testing, for each candidate pixel vector, which other pixel vectors are sufficiently similar in spectral sense. Instead of using a manual procedure as recommended by the authors in,[11] we have used the OSP technique in order to derive a final set of spectrally distinct endmembers, where the number of endmembers to be derived is an input parameter to the OSP algorithm.

2.4 Spatial Pre-Processing (SPP)

The SPP[12] serves as a preprocessing module which can be combined with existing spectral-based algorithms such as OSP. The method estimates, for each input pixel vector, a scalar factor which is intimately related to the spatial similarity between the pixel and its spatial neighbors, and then uses this scalar factor to spatially weight the spectral information associated to the pixel. The idea behind the SPP is to center each spectral feature in the data cloud around its mean value, and then shift each feature straight towards the centroid of the data cloud. The shift is proportional to a similarity measure calculated using both the spatial neighborhood around the pixel under consideration and the spectral information associated to the pixel, but without averaging the spectral signature of the pixel. The correction is performed so that pixels located in spatially homogenous areas are expected to have a smaller displacement with regards to their original location in the data cloud than pure pixels surrounded by spectrally distinct substances. Resulting from the above operation, a modified simplex is formed, using not only spectral but also spatial information. It is important to notice that the modified simplex is mainly intended to serve as a guide for a subsequent competitive endmember extraction process, conducted in this work using the OSP algorithm. However, such modified simplex is not intended to replace the simplex in the input hyperspectral scene. To achieve this, the spatial coordinates of the endmembers extracted from the preprocessed image are retained, but the spectral signatures associated to those spatial coordinates are obtained from the original hyperspectral scene.

2.5 Region-Based Spatial Pre-Processing (RBSPP)

The RBSPP[13] also uses spatial information as a guide to exploit spectral information more effectively by adequately exploiting spatial context in adaptive fashion. This approach first adaptively searches for the most spectrally pure regions (understood as groups of several contiguous pixel vectors with similar spectral content) by using a hybrid procedure that combines unsupervised clustering and orthogonal subspace projection concepts. After estimating the number of endmembers using an agreement between the virtual dimensionality (VD)[18] and the hyperspectral signal identification by minimum error (HySime)[19] concepts, the method performs unsupervised clustering using the ISODATA algorithm[20] and finally applies the OSP algorithm to the mean spectra of the resulting regions in order to find a set of spatially representative regions with associated spectra which are both spectrally pure and orthogonal between them. Once the aforementioned region-based preprocessing has been completed, a spectral-based endmember extraction algorithm such as the OSP can now be applied to the set of pixels associated to the retained spatially connected regions to produce the final set of endmembers.

3. PROPOSED METHOD

In this section we describe the considered spatial-spectral preprocessing approach. As shown by the flowchart in Fig. 1, the proposed method consists of four steps that can be summarized as follows:
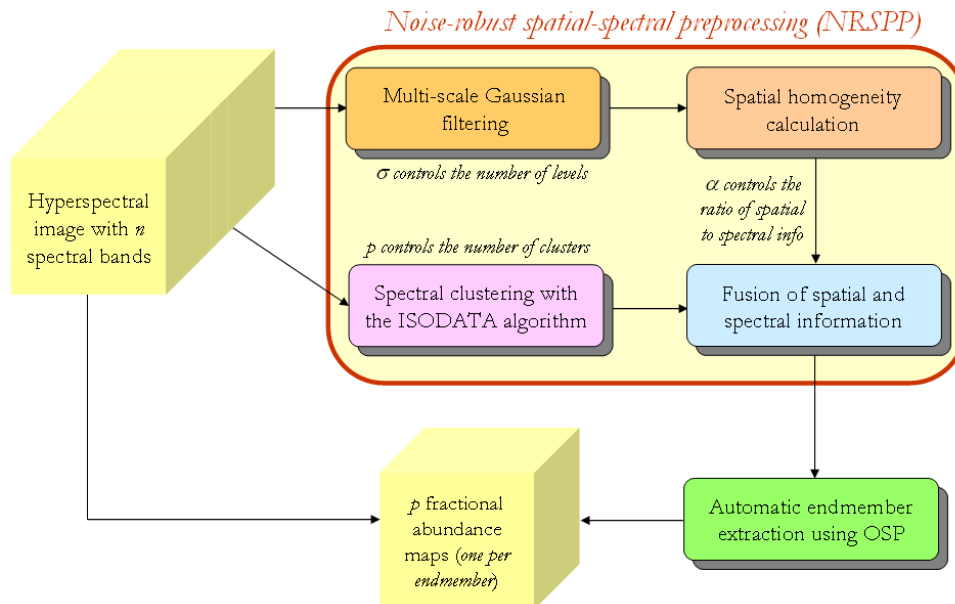
Figure 1. Block diagram illustrating a noise-robust spatial preprocessing method (NRSPP) prior to endmember extraction and spectral unmixing.

1. *Multi-scale Gaussian filtering.* First, we apply multidimensional Gaussian filtering using different values of parameter σ, which results in different filtered versions of the original hyperspectral image. Here, higher σ values lead to more spatial smoothing.

2. *Spatial homogeneity calculation.* Next, we calculate the root mean square error (RMSE)[6] between the original hyperspectral image and each of the filtered images resulting from the previous step. Then, for each pixel in the hyperspectral image we calculate a spatial homogeneity index as the average value of the corresponding values after calculating the per-pixel error scores using different values of σ.

3. *Spectral clustering.* In parallel to the first two steps, we perform a spectral-based unsupervised clustering of the original hyperspectral image. Here, we simply used the ISODATA algorithm[21] applied to a transformed version of the original image obtained using the minimum noise fraction (MNF) transform,[22] where the number of components retained was set to the number of endmembers in the input data, estimated using the virtual dimensionality (VD) concept.[18] Let us denote this value as p. Then, for the ISODATA algorithm, the minimum number of classes was set to p and the maximum number of classes was set to $2p$, which empirically resulted in good results.

4. *Fusion.* For each cluster in the spectral classification map, a subset of spatially homogeneous pixels are selected. Parameter $\alpha \in [0, 100]$ defines the percentage of pixels that will be selected per cluster. For selection, pixels are ranked according to increasing values of their spatial homogeneity as calculated in the previous step. The selected pixels for each cluster are now averaged, then we apply the OSP algorithm over the averaged signatures to select the most extreme clusters and remove the clusters with mixed pixels.

Finally, endmember extraction is applied to the retained pixels after the procedure above, called NRSPP due to its robustness in the presence of noise, by assuming that every time an endmember pixel is selected from a certain cluster, all remaining pixels in the same cluster are excluded from the endmember searching process. The outcome of the process is a set of p fractional abundance maps (one per endmember).

4. EXPERIMENTS WITH SYNTHETIC DATA

A database of five 100×100-pixel synthetic hyperspectral scenes has been created using fractals to generate distinct spatial patterns. Several natural objects can be approximated by fractals to a certain degree, including
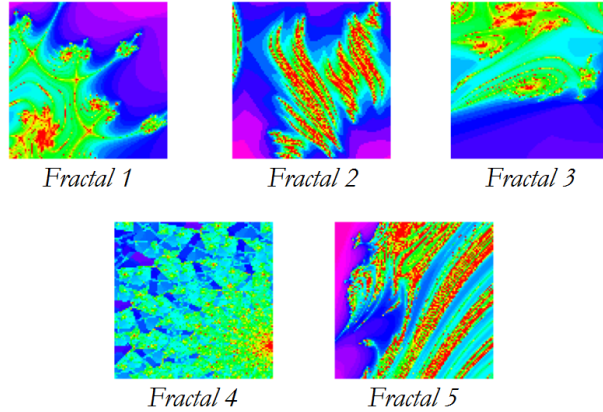
Figure 2. Synthetic images used in experiments, where spatial patterns were generated using fractals.

clouds, mountain ranges, coastlines, vegetables, etc. thus providing a baseline for simulating spatial patterns often found in nature. In this work, we used fractals to simulate linear mixtures of a set of endmember signatures randomly selected from a spectral library compiled by the U.S. Geological Survey (USGS)[*] and made up of a total of 420 signatures. Fig. 2 displays the five fractal images used in the simulations. These images are further divided into a number of clusters using the k-means algorithm,[23] where the number of clusters extracted from the five fractal images was always larger than the number of endmember signatures, fixed in our experiments to $p = 9$, and the abundance proportions in the regions associated to each cluster have been set so that pixels closer to the border of the region are more heavily mixed, while the pixels located at the center of the region are more spectrally pure in nature (the images does not contain any completely pure pixels, a situation often encountered in real-world analysis scenarios). Zero-mean Gaussian noise was added to the synthetic scenes in different signal to noise ratios (SNRs) –from 30:1 to 110:1– to simulate contributions from ambient and instrumental sources, following the procedure described in.[14] Fig. 3 shows the spectra of the USGS signatures used in the simulation of one of the synthetic scenes (labeled as "Fractal 1" in Fig. 2). The full database of synthetic scenes is available online[†]. The abundance maps associated to each reference USGS signature in the construction of the "Fractal 1" synthetic scene are also displayed in Fig. 3, where the fractional abundances in each pixel of the scene are positive and add up to unity, ensuring that all pixel instances in the synthetic fractal image strictly adhere to a fully constrained linear mixture model.[7]

In order to illustrate the performance of the proposed NRSPP, we show the individual outcome of each processing step for the "Fractal 1" in Fig. 2. Fig. 4 shows the outcome of applying Gaussian filtering with different values of σ for the synthetic image simulated with SNR=70:1. Figs. 5(a-c) respectively show the outcome of calculating the RMSE between the original image and the images obtained after Gaussian filtering in Fig. 4. Figs. 5(d-h) respectively show the spatial homogeneity images obtained for the synthetic image with SNR values ranging between 30:1 and 110:1. As shown by Figs. 5(d-h), the spatial homogeneity calculation is robust in the presence of noise. Fig. 5(i) shows the outcome of the unsupervised clustering procedure with ISODATA for the synthetic image with SNR=70:1. Finally, Figs. 5(j-n) shows the clusters (obtained after applying spatial-spectral fusion) from the image with SNR=70:1 after considering values of α from 50 to 90.

Table 1 shows the RMSE scores after reconstructing the synthetic scene (simulated with different SNR values) using the endmembers extracted by several methods, including the spectral-based OSP, several preprocessing versions applied prior to OSP (SPP, RBSPP and NRSPP), and two spatial-spectral endmember extraction algorithms (AMEE and SSEE). In our experiments, we always derive $p = 9$ endmembers using the different tested methods and then estimate their fractional abundances in the original hyperspectral image using fully constrained linear spectral unmixing (FCLSU).[7] Then, we reconstruct the original image using the derived endmembers and fractional abundances, and measure the error with regards to the original hyperspectral scene using RMSE. Table 1 indicates that the NRSPP provides the best overall results (lower RMSE values) across all
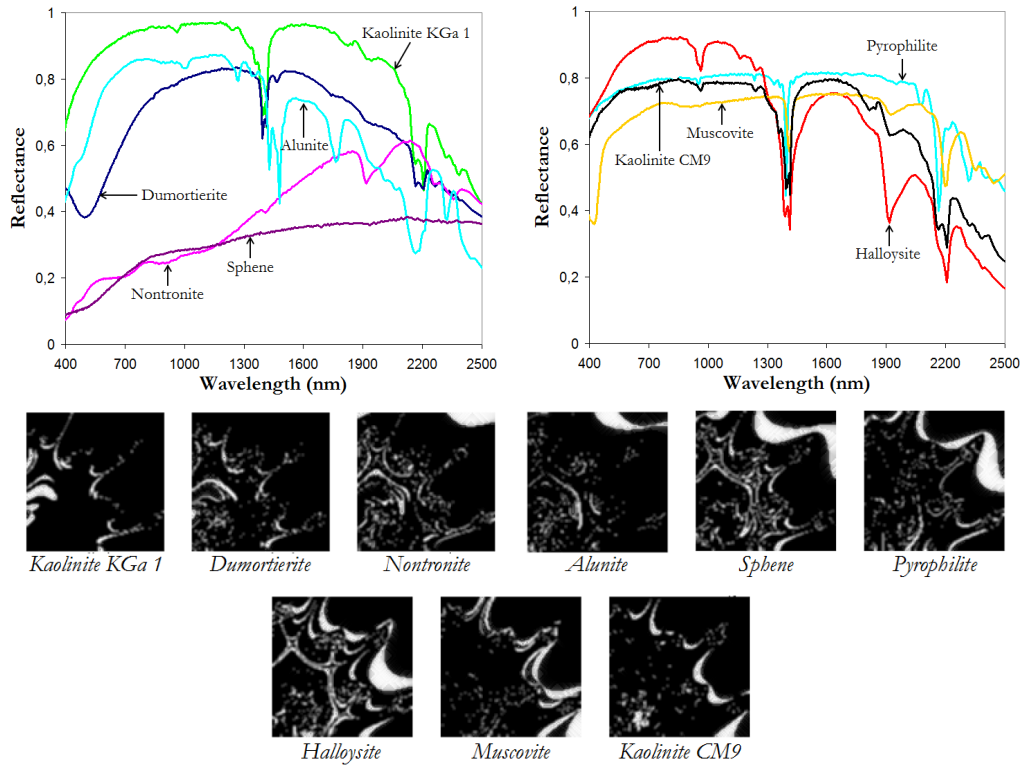

Figure 3. USGS library signatures (top) and fractional abundance distributions (bottom) considered for generating the simulated hyperspectral scene labeled as "Fractal 1" in experiments.
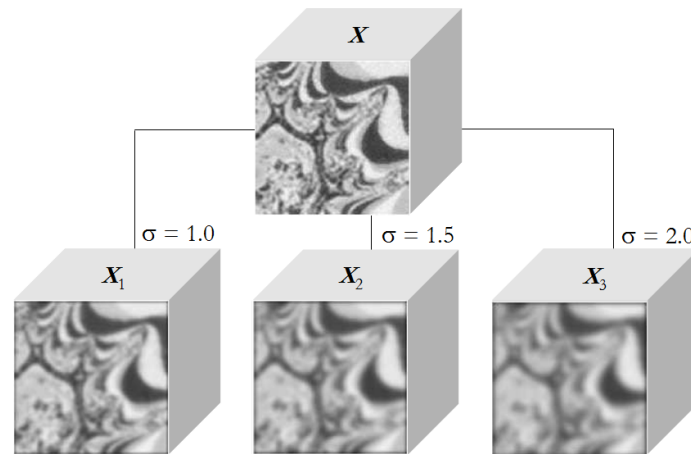

Figure 4. Gaussian filtering of the synthetic hyperspectral image "Fractal 1" in Fig. 3

Table 1. RMSE scores measured after applying several endmember extraction algorithms to the "Fractals 1" synthetic scene in Fig. 3.

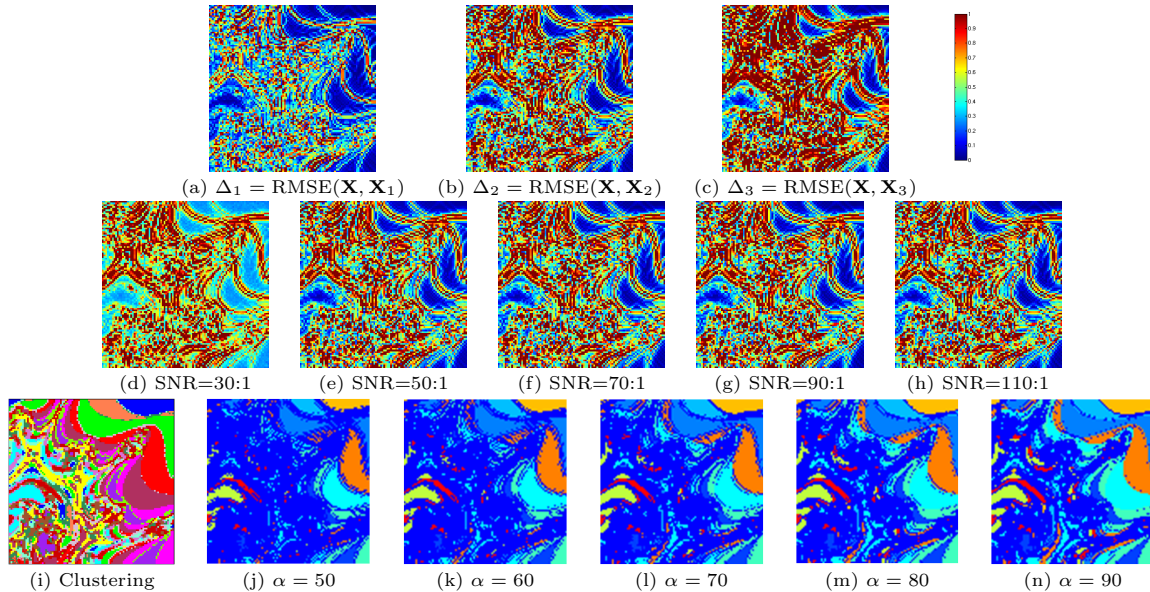| Algorithm	SNR=30:1	SNR=50:1	SNR=70:1	SNR=90:1	SNR=110:1
OSP	0.3469	0.0372	0.0084	0.0066	0.0063
SPP+OSP	0.3498	0.0423	0.0149	0.0132	0.0132
RBSPP+OSP	0.3469	0.0372	0.0087	0.0070	0.0059
NRSPP+OSP	**0.3464**	**0.0363**	**0.0068**	**0.0050**	**0.0047**
AMEE	0.4767	0.3294	0.3190	0.3187	0.3187
SSEE	0.3472	0.0439	0.0075	0.0282	0.0090

Figure 5. (a-c) Outcome of calculating the RMSE between the original synthetic image and the images obtained after Gaussian filtering in Fig. 4. (d-h) Spatial homogeneity scores for different SNR values. (i) Spectral clustering of the image with SNR=70:1. (j-n) Regions obtained after fusing (f) and (i) considering different values of α.

tested methods, regardless of the considered SNR in the simulation. This is due to the fact that the endmembers extracted by this method are more spatially representative, thus leading to better unmixing accuracy and lower per-pixel reconstruction errors.

5. EXPERIMENTS WITH REAL DATA

In this experiment we use the well-known AVIRIS Cuprite data set, available online in reflectance units[‡] after atmospheric correction. This scene has been widely used to validate the performance of endmember extraction algorithms. The portion used in experiments corresponds to a 350×350-pixel subset of the sector labeled as f970619t01p02_r02_sc03.a.rfl in the online data. The scene comprises 224 spectral bands between 0.4 and 2.5 μm, with full width at half maximum of 10 nm and spatial resolution of 20 meters per pixel. Prior to the analysis, several bands were removed due to water absorption and low SNR in those bands, leaving a total of 192 reflectance channels to be used in the experiments. The Cuprite site is well understood mineralogically,[24] and has several exposed minerals of interest included in the USGS spectral library. A few selected spectra from the USGS library, corresponding to highly representative minerals in the Cuprite mining district, are used in this work to substantiate endmember signature purity.

Fig. 6 shows the error maps obtained after reconstructing the AVIRIS Cuprite scene using $p = 19$ endmembers extracted by different methods (this value of p was estimated using a consensus between the VD and HySime concepts). The parameters of all tested methods were optimized empirically and we only report the best results obtained. For instance, in the NRSPP the optimal values were $\alpha = 70$ and σ was set to the same values used in Fig. 4 for the synthetic image experiments. Fig. 6 reveals that the application of NRSPP as preprocessing results in more robust reconstruction results than those found by using other methods due to the improved spatial representativeness of the derived endmembers and to the better characterization of noise, which results in lower per-pixel reconstruction errors when compared to other methods.

6. CONCLUSIONS AND FUTURE RESEARCH

The incorporation of spatial information in hyperspectral unmixing is a desirable goal which can better model spectral variability observed in natural scenes. In this paper, we have developed a noise-robust spatial-spectral

---

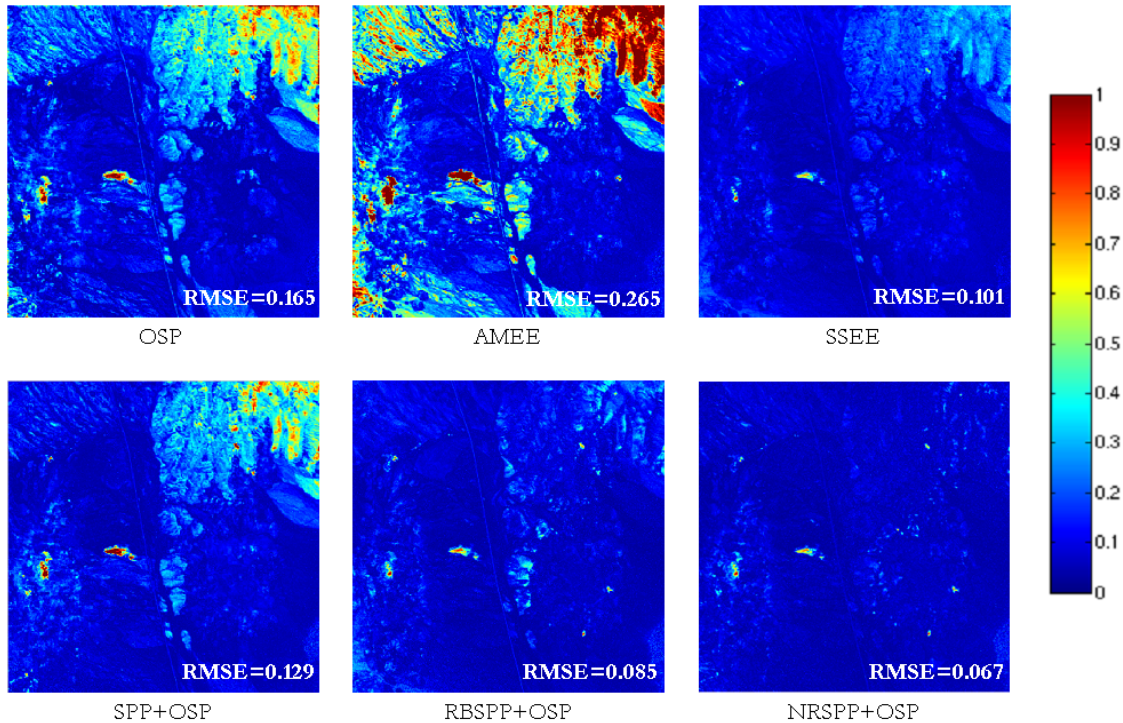[‡]http://aviris.jpl.nasa.gov/html/aviris.freedata.html

Figure 6. Errors measured for various endmember extraction algorithms after reconstructing the AVIRIS Cuprite scene.

preprocessing method which can be used prior to endmember extraction and spectral unmixing of remotely sensed hyperspectral images. It considers spatial and spectral information simultaneously and fuses both sources of information at the preprocessing level. The proposed method shows some advantages over other existing approaches, in particular, when the noise level in the hyperspectral data is relatively high. Additional experiments exploring the combined use of prescreening methods to filter out mixed pixels prior to applying the proposed method will be conducted in future research, as well as tests with more endmember extraction algorithms and hyperspectral scenes.

ACKNOWLEDGEMENT

REFERENCES

1. A. F. H. Goetz, G. Vane, J. E. Solomon, and B. N. Rock, "Imaging spectrometry for Earth remote sensing," *Science* **228**, pp. 1147–1153, 1985.
2. A. Plaza, J. A. Benediktsson, J. Boardman, J. Brazile, L. Bruzzone, G. Camps-Valls, J. Chanussot, M. Fauvel, P. Gamba, J. Gualtieri, M. Marconcini, J. C. Tilton, and G. Trianni, "Recent advances in techniques for hyperspectral image processing," *Remote Sensing of Environment* **113**, pp. 110–122, 2009.
3. M. E. Schaepman, S. L. Ustin, A. Plaza, T. H. Painter, J. Verrelst, and S. Liang, "Earth system science related imaging spectroscopy – an assessment," *Remote Sensing of Environment* **113**, pp. 123–137, 2009.
4. J. B. Adams, M. O. Smith, and P. E. Johnson, "Spectral mixture modeling: a new analysis of rock and soil types at the Viking Lander 1 site," *Journal of Geophysical Research* **91**, pp. 8098–8112, 1986.

5. R. O. Green, M. L. Eastwood, C. M. Sarture, T. G. Chrien, M. Aronsson, B. J. Chippendale, J. A. Faust, B. E. Pavri, C. J. Chovit, M. Solis, *et al.*, "Imaging spectroscopy and the airborne visible/infrared imaging spectrometer (AVIRIS)," *Remote Sensing of Environment* **65**(3), pp. 227–248, 1998.

6. N. Keshava and J. F. Mustard, "Spectral unmixing," *IEEE Signal Processing Magazine* **19**(1), pp. 44–57, 2002.

7. D. Heinz and C.-I. Chang, "Fully constrained least squares linear mixture analysis for material quantification in hyperspectral imagery," *IEEE Trans. Geosci. Remote Sens.* **39**, pp. 529–545, 2001.

8. A. Plaza, P. Martinez, R. Perez, and J. Plaza, "A quantitative and comparative analysis of endmember extraction algorithms from hyperspectral data," *IEEE Trans. Geosci. Remote Sens.* **42**(3), pp. 650–663, 2004.

9. Q. Du, N. Raksuntorn, N. H. Younan, and R. L. King, "End-member extraction for hyperspectral image analysis," *Applied Optics* **47**, pp. 77–84, 2008.

10. A. Plaza, P. Martinez, R. Perez, and J. Plaza, "Spatial/spectral endmember extraction by multidimensional morphological operations," *IEEE Trans. Geosci. Remote Sens.* **40**(9), pp. 2025–2041, 2002.

11. D. M. Rogge, B. Rivard, J. Zhang, A. Sanchez, J. Harris, and J. Feng, "Integration of spatial–spectral information for the improved extraction of endmembers," *Remote Sensing of Environment* **110**(3), pp. 287–303, 2007.

12. M. Zortea and A. Plaza, "Spatial preprocessing for endmember extraction," *IEEE Trans. Geosci. Remote Sens.* **47**, pp. 2679–2693, 2009.

13. G. Martin and A. Plaza, "Region-based spatial preprocessing for endmember extraction and spectral unmixing," *IEEE Geoscience and Remote Sensing Letters* **8**, pp. 745–749, 2011.

14. J. C. Harsanyi and C.-I. Chang, "Hyperspectral image classification and dimensionality reduction: An orthogonal subspace projection," *IEEE Trans. Geosci. Remote Sens.* **32**(4), pp. 779–785, 1994.

15. H. Ren and C.-I. Chang, "Automatic spectral target recognition in hyperspectral imagery," *IEEE Trans. on Aerospace and Electronic Systems* **39**(4), pp. 1232–1249, 2003.

16. A. Plaza, P. Martinez, J. Plaza, and R. Perez, "Dimensionality reduction and classification of hyperspectral image data using sequences of extended morphological transformations," *IEEE Trans. Geosci. Remote Sens.* **43**(3), pp. 466–479, 2005.

17. C.-I. Chang, *Hyperspectral Imaging: Techniques for Spectral Detection and Classification*, Kluwer Academic/Plenum Publishers: New York, 2003.

18. C.-I. Chang and Q. Du, "Estimation of number of spectrally distinct signal sources in hyperspectral imagery," *IEEE Trans. Geosci. Remote Sens.* **42**(3), pp. 608–619, 2004.

19. J. M. Bioucas-Dias and J. M. P. Nascimento, "Hyperspectral subspace identification," *IEEE Trans. Geosci. Remote Sens.* **46**(8), pp. 2435–2445, 2008.

20. J. A. Richards, "Analysis of remotely sensed data: the formative decades and the future," *IEEE Trans. Geosci. Remote Sens.* **43**, pp. 422–432, 2005.

21. J. A. Richards and X. Jia, *Remote Sensing Digital Image Analysis: An Introduction*, Springer, 2006.

22. A. A. Green, M. Berman, P. Switzer, and M. D. Craig, "A transformation for ordering multispectral data in terms of image quality with implications for noise removal," *IEEE Trans. Geosci. Remote Sens.* **26**, pp. 65–74, 1988.

23. J. A. Hartigan and M. A. Wong, "Algorithm as 136: A k-means clustering algorithm," *Journal of the Royal Statistical Society, Series C (Applied Statistics)* **28**, pp. 100–108, 1979.

24. G. Swayze, R. N. Clark, F. Kruse, S. Sutley, and A. Gallagher, "Ground-truthing AVIRIS mineral mapping at Cuprite, Nevada," *Proc. JPL Airborne Earth Sci. Workshop* , pp. 47–49, 1992.